Structural and Physiologic Determinants of Human Erythrocyte Sugar Transport Regulation by Adenosine Triphosphate†

Kara B. Levine, Erin K. Cloherty, Nancy J. Fidyk, and Anthony Carruthers*

Department of Biochemistry and Molecular Biology, University of Massachusetts Medical School, 55 Lake Avenue North, Worcester, Massachusetts 01655

Received March 17, 1998; Revised Manuscript Received July 9, 1998

ABSTRACT: Human erythrocyte sugar transport is mediated by the integral membrane protein GLUT1 and is regulated by cytosolic ATP [Carruthers, A., and Helgerson, A. L. (1989) *Biochemistry 28*, 8337−8346]. This study asks the following questions. (1) Where is the GLUT1 ATP binding site? (2) Is ATP−GLUT1 interaction sufficient for sugar transport regulation? (3) Is ATP modulation of transport subject to metabolic control? GLUT1 residues 301−364 were identified as one element of the GLUT1 ATP binding domain by peptide mapping and N-terminal sequence analysis of proteolytic fragments of azidoATP-photolabeled GLUT1. Nucleotide binding and sugar transport experiments undertaken with dimeric and tetrameric forms of GLUT1 indicate that only tetrameric GLUT1 binds and is subject to modulation by ATP. Reconstitution experiments indicate that nucleotide and tetrameric GLUT1 are sufficient for ATP modulation of sugar transport. Feedback control of GLUT1 regulation by ATP was investigated by measuring sugar uptake into erythrocyte ghosts containing or lacking ATP and glycolytic intermediates. Only AMP and ADP modulate ATP regulation of transport. Reduced cytosolic pH inhibits ATP modulation of GLUT1-mediated 3OMG uptake and increases $K_{d(app)}$ for ATP interaction with GLUT1. We conclude that tetrameric but not dimeric GLUT1 is subject to direct regulation by cytosolic ATP and that this regulation is antagonized by intracellular AMP and acidification.

The facilitated diffusion of sugars across cell membranes is mediated by a family of integral membrane proteins called glucose transporters or carriers. Five vertebrate, glucose carrier isoforms (GLUT1−GLUT5)[1] have been characterized (*1*), but as many as 70 related prokaryotic and lower eukaryotic gene products are now known to exist (Swiss-Protein Database).

Vertebrates maintain serum glucose levels and deliver glucose to tissues at rates commensurate with glucose utilization. In cells where protein-mediated sugar transport is rate-limiting for sugar utilization, sugar transport and sugar metabolism are regulated coordinately (*2*). Thus, cardiac and skeletal muscle and nucleated erythrocytes respond to work, anoxia, and inhibition of oxidative metabolism with acute stimulation of glycolysis and protein-mediated sugar transport (*3*−*8*).

Sugar transport stimulation in skeletal muscle by anoxia and contractile activity appears to result from translocation of the glucose transport protein GLUT4 from an intracellular compartment to the cell membrane (*9*, *10*). Recent studies also suggest that muscle contains a pool of conformationally masked GLUT4 that becomes exposed during transport stimulation (*11*). Two major glucose transporter isoforms, GLUT1 and GLUT4, are expressed in cardiac muscle, and both proteins are translocated from an intracellular compartment to the cell surface in response to ischemia, hypoxia, or contractile activity (*12*−*15*). It is not yet certain whether transport stimulation in heart muscle results from transporter recruitment alone or in combination with cell surface transporter activation. GLUT1 and GLUT4 are abundant at the cardiomyocyte surface under basal conditions, and quantitations of transport stimulation and carrier recruitment to the cell membrane are equivocal (*3*, *14*−*16*). Sugar transport in nucleated, avian erythrocytes is mediated by GLUT1 which is present only at the cell surface (*17*). Under basal conditions, avian red cell GLUT1 is incapable of uniport but catalyzes futile self-exchange of sugar (*18*). Following exposure to metabolic poisons, however, avian erythrocyte GLUT1 mediates sugar uniport, resulting in stimulation of net sugar uptake and glycolysis (*18*). Antiport (exchange transport) efficiency is unchanged by cell poisoning. The molecular mechanism of GLUT1 antiport−uniport switching is unknown, but interesting parallels can be drawn between human and avian erythrocyte sugar transport.

Human erythrocyte sugar transport is also mediated by GLUT1 (*19*, *20*) which is assembled and functions as an allosteric homotetramer (*21*, *22*). In freshly isolated erythrocytes, net uptake of 3-*O*-methylglucose (a transported but nonmetabolizable sugar) is slower by as much as 150-fold

† This work was supported by NIH Grant DK 36081.

* To whom correspondence should be addressed. E-mail: anthony.carruthers@ummed.edu. Telephone: (508) 856-5570. Fax: (508) 856-6231.

[1] Abbreviations: GLUT1, human erythrocyte glucose transport protein; 3OMG, 3-*O*-methylglucose; C-Ab, anti-GLUT1 carboxyl-terminal peptide antiserum; CB, cytochalasin B; EDTA, ethylenediaminetetraacetic acid; EggPC, egg phosphatidylcholine; EGTA, ethylene glycol bis(*β*-aminoethyl ether)-*N*,*N*,*N*′,*N*′-tetraacetic acid; HEPES, *N*-(2-hydroxyethyl)piperazine-*N*′-2-ethanesulfonic acid; HRP, horseradish peroxidase; N-Ab, anti-peptide antibodies raised against GLUT1 residues 84−96; PAGE, polyacrylamide gel electrophoresis; SDS, sodium dodecyl sulfate; Tris-HCl, tris(hydroxymethyl)aminomethane.

S0006-2960(98)00585-6 CCC: $15.00
Published on Web 08/12/1998

than 3OMG exchange transport (*23*). Following hypotonic cell lysis and cellular resealing in ATP-free medium, 3OMG net uptake (but not exchange) is stimulated by 3−10-fold (*24*). When lysed erythrocytes are resealed in ATP-containing saline, 3OMG net uptake and exchange are indistinguishable from transport observed in intact cells (*24*). This suggests that as with avian red cell sugar transport, transport stimulation in human erythrocytes results from accelerated uniport function and that cellular glucose antiport−uniport switching may be regulated by cytoplasmic ATP.

We have demonstrated that the isolated human erythrocyte glucose transport protein is also a nucleotide binding protein (*25*). ATP binding to GLUT1 promotes a GLUT1 conformational change that leaves the GLUT1 carboxyl terminus less accessible to peptide-directed antibodies. This ATP-dependent conformational change is antagonized by AMP and ADP which appear to function as competitive inhibitors of ATP binding to GLUT1. What is unclear is whether ATP binding to GLUT1 is sufficient to mediate sugar transport regulation or whether other molecular species are required (*26*). In this study, we ask the following questions. (1) Where is the GLUT1 nucleotide-binding domain? (2) What physiologic factors influence ATP modulation of sugar transport? (3) Is ATP interaction with GLUT1 sufficient for sugar transport regulation? Our findings suggest that GLUT1 residues 301−364 form an integral part of the ATP binding domain, that intracellular AMP and acidification antagonize ATP regulation of sugar transport, and that ATP interaction with GLUT1 is sufficient for transport modulation. Our findings also support the hypothesis that only tetrameric GLUT1 is regulated by ATP.

MATERIALS AND METHODS

Materials. 8-Azido[γ-^{32}P]ATP was purchased from ICN. [^{3}H]-3-*O*-Methylglucose was purchased from New England Nuclear. Rabbit antisera (C-Ab) raised against a synthetic carboxyl-terminal peptide of the rat brain glucose transport protein (residues 480−492) was obtained from East Acres Biologicals. Glycoprotein Detection Kits and ECL detection reagents were purchased from Amersham. Gradient SDS−PAGE gels were purchased from Integrated Separation Systems (Natick, MA). Nitrocellulose and Immobilon-P were obtained from Fisher Scientific. Endoproteinase Lys-C was obtained from Boehringer. All remaining materials were purchased from Sigma unless stated otherwise.

Solutions. Tris medium consisted of 50 mM Tris-HCl and 5 mM $MgCl_2$ (pH 7.4). Sample buffer (2×) contained 0.125 M Tris-HCl (pH 6.8), 4% SDS, 20% glycerol, and 50 mM DTT. KCl medium consisted of 150 mM KCl, 10 mM Tris-HCl, 5 mM $MgCl_2$, and 4 mM EGTA (pH 7.4). Stopper medium consisted of ice-cold KCl medium and 10 μM cytochalasin B, 100 μM phloretin, and 10 μM $HgCl_2$ (pH 7.4). Lysis buffer contained 10 mM Tris-HCl and 1 mM EGTA (pH 7.2). Phosphate-buffered saline (PBS) contained 140 mM NaCl, 10 mM Na_2HPO_4, 3.4 mM KCl, and 1.84 mM KH_2PO_4 (pH 7.3).

N-Terminal Antisera. A peptide corresponding to GLUT1 residues 84−96 was synthesized by the University of Massachusetts Medical School Peptide Synthesis facility. This peptide was conjugated to keyhole limpet hemocyanin using a kit purchased from Pierce. Rabbit antisera (N-Ab) against this GLUT1 peptide were obtained from Animal Pharm Services, Inc., of Healdsburg, CA. Whole IgGs were purified from crude serum by ammonium sulfate precipitation (*27*).

Red Cells. Erythrocytes were isolated from whole human blood by repeated wash−centrifugation cycles in ice-cold KCl medium. One volume of whole blood was mixed with 3 volumes of KCl medium and the mixture centrifuged at 10000*g* for 5 min at 4 °C. Serum and the buffy coat were aspirated, and the wash−centrifugation cycle was repeated until the supernatant was clear and the buffy coat was no longer visible. Cells were resuspended in 20 volumes of KCl medium, and if used in subsequent sugar transport assays, the suspensions were allowed to rest at room temperature for 30 min to deplete intracellular sugar levels.

Erythrocyte Membrane Ghosts. Washed red cells were lysed in 40 volumes lysis medium, incubated on ice for 10 min, and then centrifuged at 22000*g* for 20 min at 4 °C. The supernatant was aspirated, and the lysis−centrifugation−aspiration cycle was repeated. The resulting membranes were resealed by incubation in KCl medium at 37 °C for 60 min and harvested by centrifugation at 22000*g* for 20 min at 4 °C.

Glucose Transport Protein. Glucose transport protein was purified from human erythrocytes as described in ref *21*. The carrier is copurified with red cell lipid and is incorporated into unsealed proteoliposomes upon removal of detergent by dialysis (*28*).

Glucose Carrier Labeling with 8-Azido[γ-^{32}P]ATP. Labeling was carried out as described previously in ref *25*. Briefly, a methanolic solution of 8-azido[γ-^{32}P]ATP is dried under nitrogen and resuspended in 500 μL of Tris medium at pH 8.5 (90 μCi ^{32}P, 10 μM final azidoATP concentration). Purified GLUT1 proteoliposomes (500 μg of protein) are sedimented by centrifugation at 14000*g* for 20 min and combined with the methanol-free 8-azido[γ-^{32}P]ATP solution. The suspension is incubated on ice for 30 min, by which time ATP binding to GLUT1 achieves equilibrium. Samples are placed in a plastic weigh boat on ice and irradiated for 90 s at 280 nm in a Rayonet Photochemical Reactor. Following UV irradiation (photolabeling), GLUT1 is washed three times to remove unbound 8-azido[γ-^{32}P]ATP by centrifugation (100000*g* for 15 min) and resuspended in 10 mL of Tris medium at pH 8.5. The effects of pH on azidoATP binding to GLUT1 were examined by varying the pH of the Tris medium over the range 5.5−8.5 during photolabeling. $MgCl_2$ was present at 5 mM in all experiments reported in this study.

Glycoprotein Detection. 8-Azido[γ-^{32}P]ATP-photolabeled GLUT1 carbohydrate was detected using the Amersham ECL Glycoprotein Detection Kit. Briefly, peptide oligosaccharides are oxidized using 10 mM sodium metaperiodate and then labeled using 0.55 mM biotin hydrazide. Subsequent detection of biotinylated glycoprotein employs standard Western blotting techniques using streptavidin−horseradish peroxidase (1:10000) and ECL chemiluminescence.

Proteolysis of the Labeled Carrier. 8-Azido[γ-^{32}P]ATP- and/or biotin-labeled GLUT1 was sedimented by centrifugation at 14000*g* for 20 min and resuspended in sample buffer with or without α-chymotrypsin, endoproteinase Lys-C, or endoproteinase Glu-C (20:1 protein:enzyme by weight). Proteolysis was allowed to proceed for 30 min at 37 °C and

was arrested by addition of phenylmethyanesulfonyl fluoride (PMSF, 0.2 mM). Resulting GLUT1 fragments were separated by gradient gel electrophoresis (10 to 20% polyacrylamide−SDS gels) and transferred to nitrocellulose membranes for autoradiography and Western blotting.

Polyacrylamide Gel Electrophoresis. Proteins were resolved on 10% acrylamide gels as described in ref *29*, or where separation of proteolytic fragments was required, gradient gel electrophoresis (10 to 20% polyacrylamide gradients) was employed.

Western Blotting. Proteolytic fragments containing GLUT1 carboxyl-terminal residues 480−492 and/or GLUT1 N-terminal residues 88−95 were detected by Western blot analysis. Peptides separated by SDS−PAGE were transferred electrophoretically to nitrocellulose or Immobilon membranes which were subsequently blocked for 1 h in PBS containing 10% Carnation nonfat dry milk. Following three 5 min washes in PBS, membranes were incubated for 1 h in primary antibody (C-Ab or N-Ab) diluted 1:1000 in PBS containing 2% nonfat dry milk. Following three wash cycles to remove primary antibody, membranes were exposed for 45 min to secondary antibody (protein A−horseradish peroxidase conjugate) diluted 1:3000 in PBS containing 2% nonfat dry milk. Detection of antigen−antibody−protein A complexes was achieved by chemiluminescence using Amersham ECL reagents.

Protein Sequencing. 8-Azido[γ-^{32}P]ATP-labeled GLUT1 (100 μg) was sedimented by centrifugation at 14000*g* for 20 min and then resuspended in 0.1% SDS/Tris-HCl (pH 7.4) with or without 5 μg of endoproteinase Lys-C. Digestion was carried out for 18−24 h at 4 °C. GLUT1 fragments were separated using 1 mM thioglycolate pre-equilibrated gradient gels. Separated peptides were transferred electrophoretically to Immobilon-PVDF membranes, and following detection by autoradiography and/or by Coomassie blue staining, protein bands of interest were excised from the membrane, washed extensively in distilled water, and subjected to microsequence analysis by J. Leczyk of the University of Massachusetts Medical School Protein Chemistry facility.

Net 3-O-Methylglucose Uptake. Sugar-free cells or ghosts at the temperature of ice were exposed to 5 volumes of ice-cold KCl medium containing [^{3}H]-3-*O*-methylglucose and variable concentrations of unlabeled 3-*O*-methylglucose. Uptake was measured over intervals of 15 s to 1 min, and then 50 volumes (relative to cell volume) of stopper solution was added to the cell/ghost suspension. Cell/ghost suspensions were sedimented by centrifugation (14000*g* for 30 s), washed once in stopper solution, collected by centrifugation, and extracted in 500 μL of 3% perchloric acid. The acid extract was centrifuged, and duplicate samples of the clear supernatant were counted. Time zero uptake points were prepared by addition of stopper solution to cell/ghost suspensions prior to addition of medium containing sugar and radiolabel. Cell/ghost suspensions were immediately processed. Radioactivity associated with cell/ghost suspensions at time zero was subtracted from the activity associated with cell/ghost suspensions following the uptake period. All uptakes were normalized to equilibrium uptake where cell/ghost suspensions were exposed to sugar medium at 37 °C for 60 min prior to addition of stopper solution. Uptake assays were performed using solutions and tubes pre-equilibrated to 4 °C.

Effects of Glycolytic Intermediates on 3-O-Methylglucose Uptake. Glycolytic intermediates were introduced into human erythrocyte ghosts by addition to the ice-cold resealing medium prior to membrane resealing. The membranes were warmed to 37 °C for 60 min, and then resealed ghosts were harvested by centrifugation (22000*g* for 20 min at 4 °C) and washed once in 50 volumes of KCl medium to remove extracellular glycolytic intermediates. Ghosts were then processed for 3-*O*-methylglucose uptake measurements as described above.

Effects of pH on ATP Modulation of 3-O-Methylglucose Uptake. Membrane ghosts were resealed in KCl medium containing 5 mM $MgCl_2$ and ATP at varying concentrations and adjusted to a pH ranging from 5.5 to 8.0. All other solutions (uptake media and stopper) were also adjusted to the same pH. Ghosts were then processed for 3-*O*-methylglucose uptake measurements as described above.

Reconstituted GLUT1-Mediated Sugar Transport. EggPC (40 mg in hexane) and cholesterol (10 mg) (≈80:20 molar ratio) were dissolved in hexane. The organic phase was evaporated under a stream of N_2, and remaining trace quantities of hexane were removed in vacuo for 3 h. The resulting lipid film was dissolved in Tris medium containing 5% (by weight) sodium cholate and mixed with 100 μg of GLUT1 solubilized in 50 mM sodium cholate. This mixture (4 mL) was dialyzed overnight against 6 L of detergent-free Tris medium, and the resulting suspension of small unilamellar proteoliposomes was distributed in 0.5 mL fractions in microcentrifuge tubes. Each tube was frozen in a dry ice/isopropyl alcohol mixture, thawed at room temperature, and then subjected to two additional rounds of freezing and thawing. The resulting large unilammelar proteoliposomes (mean diameter of 2.5 μm by oil immersion phase contrast) sedimented readily at 14000*g* and were used for sugar transport determinations at 24 °C. 3OMG uptake (0.05 mM) was measured in 100 μL of proteoliposome suspension (2 μg of GLUT1) at 0, 10, 20, 30, and 60 s in Tris medium with or without 10 μM CB [a transport inhibitor; $K_{i(app)} = 0.2$ μM]. Equilibrium uptake was measured by incubation for 2 h at 24 °C. Uptake was arrested by addition of 1 mL of ice-cold Tris medium containing 10 μM CB. Proteoliposomes were sedimented by centrifugation at 14000*g* for 5 min at 4 °C; the supernatant was aspirated, and the liposomes were washed again in Tris medium containing CB. Uptake, v, was computed as

$$v = [3\mathrm{OMG}]\frac{(\mathrm{cpm}_t - \mathrm{cpm}_0)}{(\mathrm{cpm}_\infty - \mathrm{cpm}_0)t}$$

where t is time and cpm_0, cpm_t, and cpm_∞ correspond to radioactivity associated with proteoliposomes at time zero, time t, and equilibrium.

Calculation of Mg^{2+} and ATP Levels. In some GLUT1 photolabeling experiments, pH and ATP concentration were varied systematically at fixed EGTA (4 mM) and $MgCl_2$ (5 mM) levels. Exogenous $CaCl_2$ was not added; thus, total Ca levels were limited to Ca contamination (approximately 15 μM; *24*). Computation of Mg^{2+}, Mg_2·ATP, Mg_2H·ATP, ATP, Mg_2·EGTA, Mg_2H·EGTA, and EGTA levels was carried out using the WinMaxC program (*30*) and equilib-

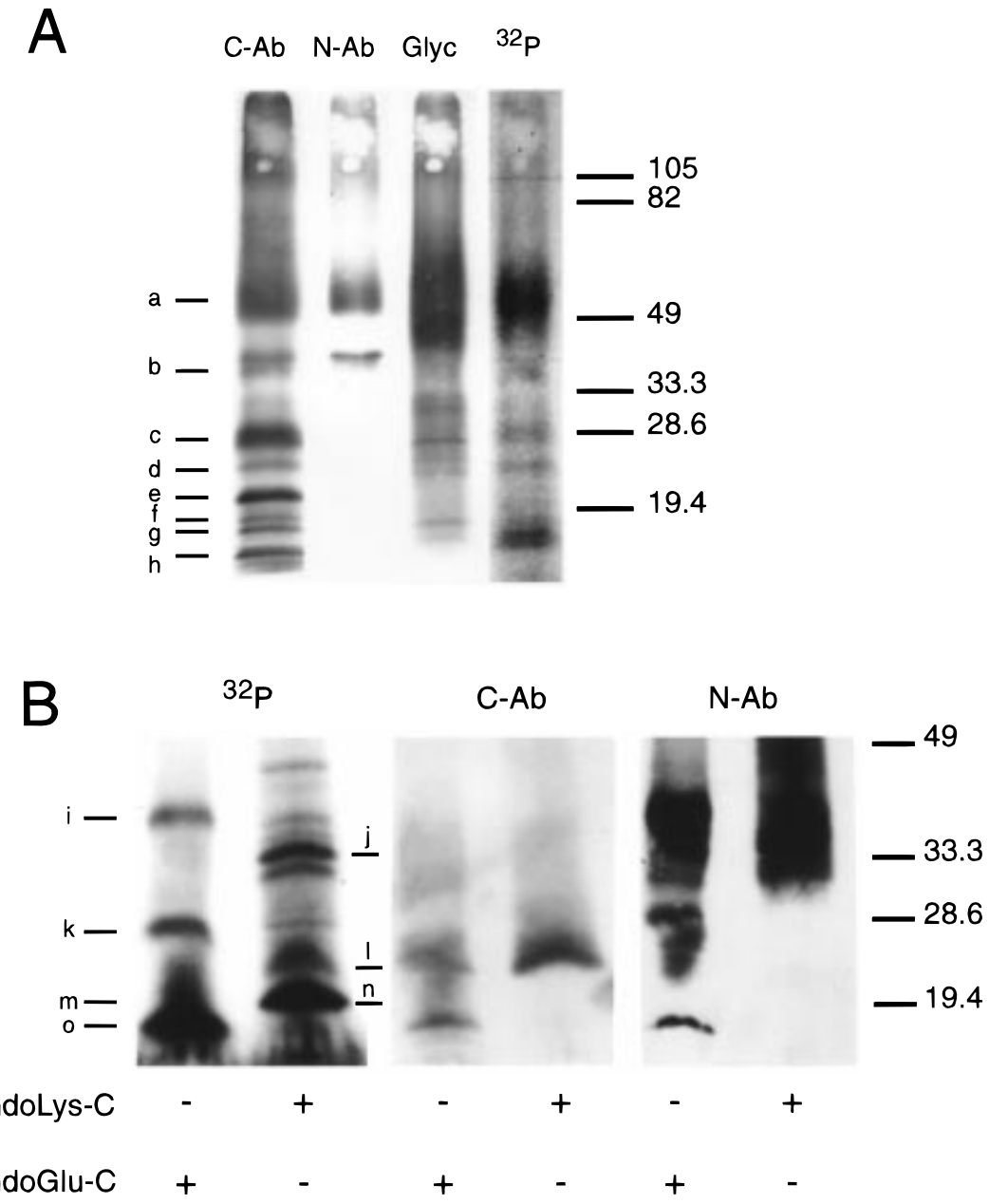

FIGURE 1: Peptide mapping of photolabeled GLUT1. (A) Purified GLUT1 (40 μg and biotinylated on carbohydrate residues) was photolabeled using 10 μM azido[γ-^{32}P]ATP and then incubated in sample buffer containing 5 μg of chymotrypsin (30 min at 37 °C). Peptides were separated on a 10 to 20% SDS−PAGE gradient gel and transferred to nitrocellulose. [γ-^{32}P]ATP-containing peptides were detected by autoradiography (^{32}P). C-Ab- and N-Ab-reactive peptides were detected using immunoblot analysis. Biotinylated carbohydrate (Glyc) was detected by stretptavidin blot analysis. C-Ab, N-Ab, ^{32}P, and Glyc analyses were performed on a single common lane of electrophoretically separated peptides. Major peptides were assigned a label (**a**−**h**) and are indicated by the left-most solid bars. The mobilities and M_r values of molecular mass standards are indicated by the solid bars to the right of the figure. (B) EndoLys-C digestion and sequencing of azido-[γ-^{32}P]ATP-photolabeled GLUT1. Labeled, purified GLUT1 (100 μg) was incubated in 0.1% SDS and 50 mM Tris-HCl medium (pH 7.4) containing 5 μg of endoproteinase Lys-C (EndoLys-C; 18−24 h at 4 °C) or 5 μg of endoproteinase Glu-C (EndoGlu-C; 1 h at 37 °C). Peptides were separated on a 10 to 20% SDS−PAGE gradient gel which had been pre-equilibrated with 1 mM thioglycolate and subsequently transferred to Immobilon-PVDF for staining with Coomassie blue. Bands containing [γ-^{32}P]ATP were identified by autoradiography (^{32}P). C-Ab- and N-Ab-reactive peptides were detected using chemiluminescence immunoblot analysis. Major peptides were assigned a label (**i**−**o**) and are indicated by the left-most solid bars. The mobilities and M_r values of molecular mass standards are indicated by the solid bars to the right of the figure. An intensely labeled 19 kDa band (peptide **n**) was excised from the membrane, washed 10 times with distilled water, and subjected to sequence analysis by the University of Massachusetts Medical Center Microsequencing Facility. A single sequence was obtained as AGVQQPVYAT corresponding to GLUT1 residues 301−310.

rium constants cited by Smith and Martell (*31*) for H^+, Ca^{2+}, Mg^{2+}, and K^+ interaction with EGTA and ATP adjusted for pH and temperature (4 °C). The apparent dissociation constants (−log) calculated for EGTA and ATP at pH 5.5 are $K_{ATPCa} = 2.91$, $K_{ATPMg} = 2.91$, $K_{EGTACa} = 3.30$, and $K_{EGTAMg} = -0.31$; at pH 6 are $K_{ATPCa} = 3.32$, $K_{ATPMg} = 3.33$, $K_{EGTACa} = 4.30$, and $K_{EGTAMg} = 0.19$; at pH 7 are $K_{ATPCa} = 3.88$, $K_{ATPMg} = 3.89$, $K_{EGTACa} = 6.29$, and $K_{EGTAMg} = 1.22$; at pH 8 are $K_{ATPCa} = 4.02$, $K_{ATPMg} = 4.03$, $K_{EGTACa} = 8.27$, and $K_{EGTAMg} = 2.39$; and at pH 8.5 are $K_{ATPCa} = 4.03$, $K_{ATPMg} = 4.04$, $K_{EGTACa} = 9.22$, and $K_{EGTAMg} = 3.10$. Our calculations confirm that Mg^{2+} levels decline linearly over

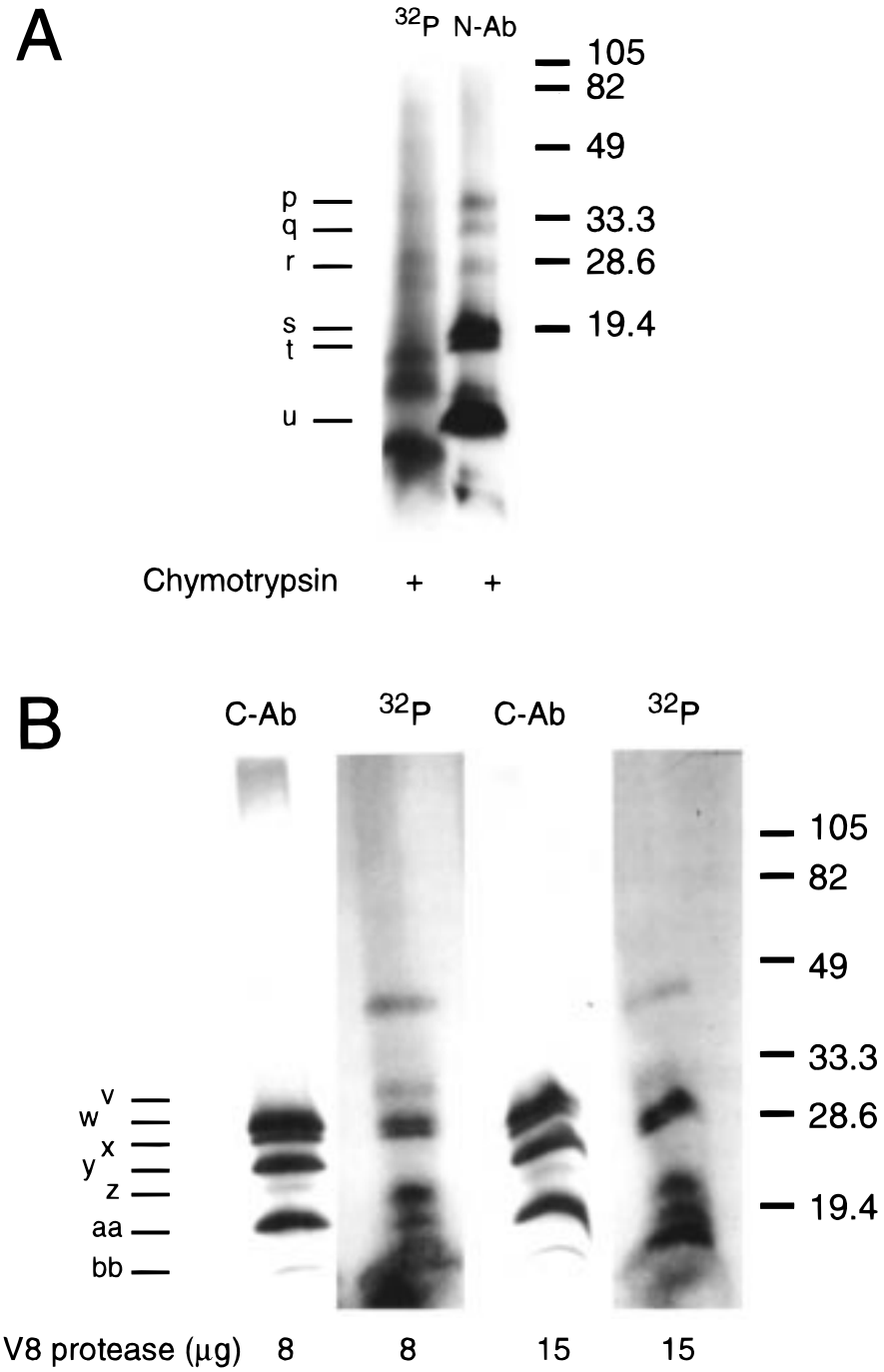

FIGURE 2: Peptide mapping of photolabeled GLUT1. (A) Purified GLUT1 (40 μg) was photolabeled using 10 μM azido[γ-^{32}P]ATP and then incubated in sample buffer containing 5 μg of chymotrypsin (30 min at 37 °C). Peptides were separated on a 10 to 20% SDS−PAGE gradient gel and transferred to nitrocellulose. [γ-^{32}P]ATP-containing peptides were detected by autoradiography (^{32}P). N-Ab-reactive peptides were detected using immunoblot analysis. Major peptides were assigned a label (**p**−**u**) and are indicated by the left-most solid bars. The mobilities and M_r values of molecular mass standards are indicated by the solid bars to the right of the figure. (B) V8 protease digestion of azido[γ-^{32}P]ATP-photolabeled GLUT1. Labeled, purified GLUT1 (100 μg) was incubated in 0.1% SDS and 50 mM Tris-HCl medium (pH 7.4) containing 8 or 15 μg of endoproteinase Glu-C (EndoGlu-C; 1 h at 37 °C). Peptides were separated on a 10 to 20% SDS−PAGE gradient gel and subsequently transferred to Immobilon-PVDF for staining with Coomassie blue. Bands containing [γ-^{32}P]ATP were identified by autoradiography (^{32}P). C-Ab-reactive peptides were detected using chemiluminescence immunoblot analysis. Major peptides were assigned a label (**v**−**bb**) and are indicated by the left-most solid bars. The mobilities and M_r values of molecular mass standards are indicated by the solid bars to the right of the figure.

the pH range of 5.5−8.5 (from 2.4 to 0.5 mM) due to increasing chelation by EGTA and variable association with ATP. Mg_2ATP and Mg_2HATP levels increase from 2.85 mM at pH 5.5 to a peak of 3.5 mM at pH 7.0 and therafter decline to 3.2 mM at pH 8.5. Free ATP levels are greatest at pH 5.5 (1.4 mM), are lowest at pH 7 (0.4 mM), and thereafter increase to 0.8 mM at pH 8.5.

Computation of Transport and Labeling Constants. In some experiments, transport rates and GLUT1 labeling by ATP were shown to change in a nonlinear (saturable) manner with increasing ATP concentrations (e.g., Figure 5). In these instances, best-fit curves were generated by nonlinear regression using the software package KaleidaGraph 3.08d (Synergy Software, Reading, PA) and assuming the following

relationships.

In Figure 5A at pH 8, the rate of uptake $= k_1 + k_2[\text{ATP}]/(K_{\text{dATP}} + [\text{ATP}])$, where k_1 is the basal transport rate in the absence of ATP, k_2 is the increment in transport produced by saturating ATP levels, and K_{dATP} is the apparent K_d for ATP interaction with the transport system.

In Figure 5A at pH 5.5, the rate of uptake $= k_1 + k_2[\text{ATP}]/(K_{\text{dATP1}} + [\text{ATP}]) - k_3[\text{ATP}]/(K_{\text{dATP2}} + [\text{ATP}])$, where k_1, k_2, and K_{dATP1} correspond to those parameters for Figure 5A at pH 8 but where k_3 and K_{dATP2} describe an additional interaction with ATP that reduces net uptake.

In Figure 5B at pH 5.5 and 8.0, the extent of labeling $= k_4 - k_5[\text{ATP}]/(K_{\text{iATP}} + [\text{ATP}])$, where k_4 is the extent of labeling in the absence of unlabeled ATP, k_5 is the decrease in labeling produced by saturating ATP levels, and K_{iATP} is the concentration of ATP that inhibits labeling half-maximally.

RESULTS

Peptide Mapping of the GLUT1 ATP Binding Site

Previous studies from this laboratory have demonstrated that GLUT1 and azidoATP associate reversibly to form a binary complex and that azidoATP binding to GLUT1 is inhibited competitively by ATP, ADP, and AMP (*25*). UV irradiation of the azidoATP−GLUT1 complex activates the ATP azido group, resulting in covalent attachment of a bound nucleotide to GLUT1. Limited proteolysis studies suggest that the point of photoattachment of azidoATP to GLUT1 falls within the carboxyl-terminal half of the protein (residues 270−456; *25*). We have now undertaken more detailed peptide mapping analyses to define more precisely the site of covalent attachment of the nucleotide to GLUT1.

Peptide mapping studies of integral membrane proteins such as GLUT1 are complicated by the typically hydrophobic nature (high SDS binding capacity) of the resulting peptides and by the presence of an N-linked oligosaccharide. For example, human erythrocyte band 7 proteins include the multi-spanning integral membrane glycoproteins aquaporin (28 kDa) and RhD ($M_r = 45$ kDa) (*32*) but are resolved as a 32 kDa protein band upon 10% SDS−PAGE (*22*). Intact GLUT1 ($M_r = 55$ kDa) is resolved as a 50 kDa band (Figure 1A). We therefore resolved to use GLUT1 internal markers to assist in peptide identification. Peptides containing an N-linked oligosaccharide (Asn45) were identified by blot analysis (using streptavidin-conjugated HRP) of GLUT1 fragments obtained from glucose transporter biotinylated on carbohydrate residues prior to proteolysis. Peptides containing GLUT1 residues 84−96 (N residues) and/or 480−492 (C residues) were identified by use of rabbit antisera (N-Ab and C-Ab, respectively) raised against synthetic peptides corresponding to these GLUT1 domains. Each experiment (see Figure 1A) thus involves biotinylation of carbohydrate exposed by unsealed GLUT1 proteoliposomes, followed by GLUT1 photolabeling using azido[γ-^{32}P]ATP. The labeled proteoliposomes are subjected to limited proteolysis; peptides are resolved by SDS−PAGE and transferred to Immobilon or nitrocellulose, and biotinylated and/or ^{32}P-labeled peptides are detected by autoradiography. The very same membrane filters are then probed for the presence of peptides containing N and C residues by chemiluminescence immunoblot analysis.

FIGURE 3: Summary of peptide mapping analysis of [γ-^{32}P]ATP-labeled GLUT1 (Figures 1 and 2). The horizontal axis represents GLUT1 residues 1−492. ^{32}P-labeled and unlabeled peptides are indicated by black and white bars, respectively. Data are from Figures 1 and 2 and are cross-referenced by peptide labels (**a**−**bb**). Peptides containing the C-Ab-reactive sequence overlap with GLUT1 residues 480−492. Peptides containing the N-Ab-reactive sequence overlap with GLUT1 residues 88−95. Peptides containing biotinylated carbohydrate also contain GLUT1 residue Asn45. When two peptides are linked by a single vertical bar, this indicates that localization is ambiguous, and the range of possibilities is shown for the linked peptides. The length of each peptide was computed by assuming that the electrophoretic mobility accurately represents the peptide molecular mass. The shaded vertical box spanning GLUT1 residues 291−364 represents that region of GLUT1 that most likely contains covalently attached [γ-^{32}P]ATP. The striped bar represents a 19 kDa, [γ-^{32}P]ATP-labeled, EndoLys-C fragment (peptide **n**) of GLUT1 whose N-terminal residue (A301) was confirmed by sequencing. Peptides **e** and **y** should (but do not) contain [γ-^{32}P]ATP and are shaded differently for comparison. Presumed specificities of proteolysis are as follows: EndoLys-C, K; V8 protease, D and E; and chymotrypsin, F, W, and Y.

Figure 1A indicates that not all N- or C-Ab-reactive peptides contain ^{32}P or biotinylated carbohydrate. Similarly, not all ^{32}P-containing peptides include N- or C-Ab-reactive sequences. Figure 1B shows EndoLys-C and EndoGlu-C (V8) digests of azido[γ-^{32}P]ATP-labeled GLUT1 which were subsequently probed for ^{32}P and C and N residues. One of the ^{32}P-labeled peptides (peptide **n**) was subjected to N-terminal sequence analysis (see below). Figure 2 summarizes additional experiments in which azidoATP-labeled, intact GLUT1 was subjected to digestion by chymotrypsin (Figure 2A) or by V8 protease (Figure 2B). Major peptides of Figures 1 and 2 have an assigned label and are aligned in Figure 3 according to size, sequence content (identified by internal markers), and assumed proteolytic specificity. This analysis permits approximate localization of the site of

covalent attachment of [γ-^{32}P]ATP to residues 291−364. Because the masses of hydrophobic and glycosylated proteins obtained by SDS−PAGE analysis are approximate, this region of nucleotide attachment should be viewed with some caution.

Two peptides have properties inconsistent with this conclusion. Peptide **e** (Figure 1A) and peptide **y** (Figure 2B) cross-react with C-Ab and are characterized by $M_{r(app)}$ values of 19.9 and 22.4 kDa, respectively, but contain no detectable ^{32}P. Three observations suggest that these peptides are dysfunctional, GLUT1 fragments present in GLUT1 proteoliposomes prior to labeling and digestion. (1) These C-Ab-reactive peptides are observed occasionally in GLUT1 preparations that are untreated by proteolytic enzymes (*21*; E. K. Cloherty and A. Carruthers, unpublished observations). (2) Peptide **y** does not correspond to any possible V8-specific GLUT1 cleavage product. (3) Peptide **n** overlaps with peptides **e** and **y**, contains ^{32}P, and is identified definitively by N-terminal sequencing (see below).

N-Terminal Microsequencing

To further refine the definition of the site of nucleotide attachment, azido[γ-^{32}P]ATP-labeled GLUT1 was subjected to endoproteinase Lys-C digestion. Endoproteinase Lys-C specifically hydrolyzes amide, ester, and peptide bonds at the carboxylic side of lysine (*33*). If it is assumed that the conditions of proteolysis reveal each cleavage site and also favor specificity, this enzyme is expected to produce a 16 kDa GLUT1 fragment corresponding to residues 301−456. Purified, azidoATP-labeled GLUT1 was exposed to EndoLys-C for 18−24 h at 4 °C, and the resulting peptides were resolved on 10 to 20% gradient SDS−PAGE gels. Following transfer to Immobilon-P membranes, the blots were exposed to film for autoradiography and stained with Coomassie blue. Bands of interest were excised from the membrane and subjected to N-terminal microsequence analysis. Figure 1B indicates that a 19 kDa band (peptide **n**) is heavily labeled by [γ-^{32}P]ATP but lacks recognition sites for both N- and C-Ab. N-terminal sequence analysis of this peptide yielded 10 pmol of a single sequence of AGVQQPVYAT corresponding to GLUT1 residues 301−310.

Factors Influencing ATP Modulation of Sugar Transport

Glycolytic Intermediates. Glycolysis and GLUT1-mediated transport appear to be regulated coordinately in certain tissues (*18*). We were intrigued by the possibility that GLUT1-mediated sugar transport might be subject to regulatory feedback mechanisms similar to those found in the glycolytic pathway.

Intracellular (but not extracellular; see ref *24*) Mg·ATP converts 3OMG transport by resealed erythrocyte ghosts from a high-capacity low-affinity transport system [$V_{max} = 1069 \pm 84$ μM/min, $K_{m(app)} = 12.3 \pm 0.8$ mM] to a low-capacity high-affinity system [$V_{max} = 220 \pm 19$ μM/min, $K_{m(app)} = 386 \pm 24$ μM, $n = 4$]. The net effect of ATP is to increase 3OMG uptake at 0.1 mM sugar by 2−5-fold (see also ref *25*). We used this simple assay of 3OMG uptake at 0.1 mM sugar to determine how resealing erythrocyte ghosts with or without glycolytic intermediates affect basal and ATP-modulated sugar transport. Table 1 shows that ATP modulation of transport is inhibited by intracellular AMP (2 mM). Extracellular AMP has no effect on basal or ATP-modulated 3OMG transport. This result is not unexpected because previous work in this laboratory has shown that AMP_i, though unable to mimic the action of ATP_i on transport, competes with ATP_i for access to the transport system (*25*). Resealing ghosts with 2 mM ADP stimulates basal transport. The remaining glycolytic intermediates have no effect on basal or ATP-modulated transport whether they are applied at the cytoplasmic or extracellular (not shown) surface of the erythrocyte membrane.

Table 1: Effects of Glycolytic Intermediates on Erythrocyte 3OMG Uptake

addition[a]	3OMG uptake (μmol L of cell water^{-1} min^{-1})	
	0 M Mg·ATP	4 mM Mg·ATP
no addition	19 ± 2	49 ± 3
AMP (2 mM)	4 ± 1	7 ± 1
ADP (2 mM)	39 ± 3	no Δ
NAD (2 mM)	no Δ[b]	no Δ
NADH (2 mM)	no Δ	no Δ
pyruvate (4 mM)	no Δ	no Δ
citrate (2 mM)	no Δ	no Δ
lactate (2 mM)	no Δ	no Δ
fructose 1,6-bisphosphate (4 mM)	no Δ	no Δ
fructose 2,6-bisphosphate (4 mM)	no Δ	no Δ
Na_2HPO_4 (4 mM)	no Δ	no Δ
2,3-diphosphoglycerate (2 mM)	no Δ	no Δ
phosphocreatine (1 mM)	no Δ	no Δ
phosphoenolpyruvate (0.1 mM)	no Δ	no Δ
fructose 6-phosphate (0.1 mM)	no Δ	no Δ
glucose 6-phosphate (0.1 mM)	no Δ	no Δ
glyceraldehyde 3-phosphate (0.1 mM)	no Δ	no Δ
2-phosphoglycerate (0.1 mM)	no Δ	no Δ
adenosine (50 μM)	no Δ	no Δ

[a] Erythrocyte ghosts were resealed in KCl medium containing 5 mM $MgCl_2$ plus the addition shown and adjusted to pH 7.4. [b] no Δ indicates that there is no significant difference between the test measurement and the measurement observed with no addition. The number of measurements per condition was three or more. Results are shown as the mean ± SEM.

Intracellular pH. The experiments describing the effects of glycolytic intermediates on basal and ATP-modulated 3OMG uptake were performed at pH 7.4. Under physiologic conditions in muscle and erythrocytes, increased glycolysis elevates cellular lactate levels, resulting in an acidosis (*34*). We therefore examined the ability of altered pH_i to modulate ATP regulation of GLUT1-mediated sugar transport. Red blood cell ghosts were resealed in KCl medium with or without 4 mM Mg·ATP adjusted to pH 5.5, 6.0, 7.0, or 8.0. Both extra- and intracellular media were adjusted to the same pH to avoid pH changes due to transmembrane proton flow. Earlier studies have demonstrated that the extracellular sugar uptake site is remarkably insensitive to alterations in external pH (*35*). KCl medium was employed in both extra- and intracellular media to avoid transmembrane KCl gradients and K^+ transport-induced volume changes.

Figure 4A shows that as pH decreases from 8.0 to 5.5, ATP modulation of 100 μM 3OMG uptake is reduced. Subsequent experiments (see Figure 5A) show even stronger inhibition of ATP-modulated transport. Basal transport rates are unaffected. Calculation of free Mg, free ATP, and Mg·ATP levels indicates that this inhibition is unrelated to systematic (pH-dependent) alterations in the ionization state of ATP (see Materials and Methods). The loss of ATP

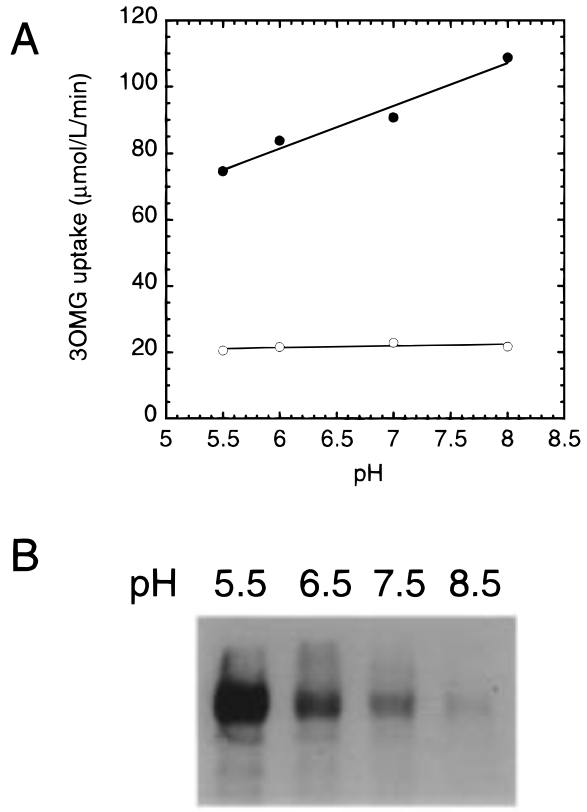

FIGURE 4: Effects of pH on ATP modulation of sugar transport (A) and GLUT1 labeling by azido[γ-^{32}P]ATP (B). (A) Erythrocytes were lysed and resealed in KCl medium containing (●) or lacking (○) 2 mM exogenous ATP. The pH of the resealing and extracellular media is shown on the abscissa. On the ordinate are the initial rates of 100 μM 3OMG uptake (micromoles per liter of cell water per minute). These results summarize triplicate measurements. Lines drawn through the data points were computed by the method of least squares. (B) Purified GLUT1 was incubated in Tris-HCl medium containing 15 μM azido[γ-^{32}P]ATP at the pH indicated for 15 min at 4 °C. Each sample was UV irradiated for 1 min and 30 μg of labeled protein resolved on 10% SDS−PAGE minigels. Peptides were transferred to nitrocellulose, and labeled bands containing [γ-^{32}P]ATP were identified by autoradiography.

modulation of transport at lower pH could result from altered binding kinetics (affinity or capacity of GLUT1 for ATP) or from the pH-dependent binding of a regulatory molecule to the ATP·GLUT1 complex. To examine these possibilities, purified GLUT1 was photolabeled at pH 5.5, 6.5, 7.5, and 8.5 with 10 μM azidoATP. Protein was separated on minigels and labeling quantitated by autoradiography. Figure 4B shows that contrary to our expectations, ATP incorporation into GLUT1 is reduced as the pH increases from 5.5 to 8.0.

To better understand this phenomenon, we measured the ATP dependence of 3OMG uptake in resealed red cell ghosts at pH 5.5 and 8.0. Figure 5A shows that 100 μM 3OMG uptake increases in a saturable manner with ATP concentration at pH 8.0. At pH 5.5, however, transport is maximally stimulated at 200 μM ATP, but is inhibited at 2 mM ATP. Figure 5B summarizes three separate experiments in which azido[γ-^{32}P]ATP labeling of GLUT1 was carried out at pH 5.5 and 8.0 in the presence of increasing concentrations of a competing unlabeled ligand, ATP. ATP inhibition of GLUT1 labeling by azidoATP shows simple competition kinetics at both pH 5.5 and 8.0, but the maximum level of labeling by azidoATP and $K_{i(app)}$ for ATP inhibition of

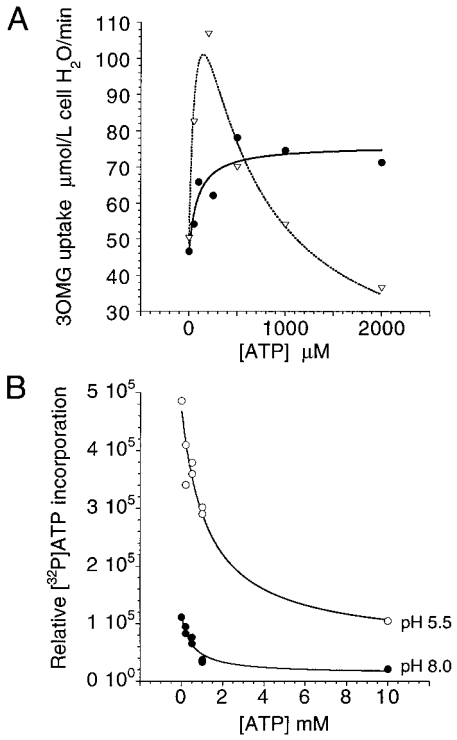

FIGURE 5: Effects of pH on the concentration dependence of ATP modulation of sugar transport (A) and ATP inhibition of GLUT1 labeling by azido[γ-^{32}P]ATP (B). (A) Erythrocytes were lysed and resealed in KCl medium containing 5 mM $MgCl_2$ and increasing concentrations of ATP at pH 8.0 (●) or 5.5 (○). On the ordinate are the initial rates of 100 μM 3OMG uptake (micromoles per liter of cell water per minute). On the abscissa is the ATP content of the resealing medium in micromolar. The results summarize three separate experiments each made in triplicate. Lines drawn through the data points were computed by nonlinear regression (see Materials and Methods). These analyses assume that ATP modulation of transport at pH 8 is comprised of basal transport (k_1 seen at 0 M ATP) and a simple, ATP-dependent Michaelis−Menten component where k_2 is the increment in transport produced by saturating ATP levels and K_{dATP} is the apparent K_d for ATP interaction with the transport system. The computed constants are as follows: $k_1 = 46$ μM/min, $k_2 = 30$ μM/min, and $K_{dATP} = 89$ μM ATP. ATP modulation of transport at pH 5.5 is similar to that at pH 8 but is characterized by an additional interaction with ATP that reduces net uptake where k_3 is the decrement in transport produced by saturating ATP levels and K_{dATP2} is the apparent K_i for ATP inhibition of transport. The computed constants are as follows: $k_1 = 48$ μM/min, $k_2 = 259$ μM/min, $K_{dATP1} = 189$ μM ATP, $k_3 = 259$ μM/min, and $K_{dATP2} = 199$ μM ATP. (B) ATP inhibition of GLUT1 photolabeling by azido[γ-^{32}P]ATP at pH 5.5 (○) and 8.0 (●). Purified GLUT1 was incubated for 15 min at 4 °C in Tris-HCl medium containing 5 mM $MgCl_2$ and 15 μM azido-[γ-^{32}P]ATP at pH 5.5 or 8.0 in the presence of increasing concentrations of ATP. Each sample was UV irradiated for 1 min and 30 μg of labeled protein resolved on 10% SDS−PAGE minigels. Peptides were transferred to nitrocellulose, and labeled bands containing [γ-^{32}P]ATP were identified by autoradiography. On the ordinate is the relative [γ-^{32}P]ATP incorporation into GLUT1 as judged by densitometric analysis of resulting autoradiograms. On the abscissa is the [ATP] during photolabeling (millimolar). These data are a summary of two separate experiments. Lines drawn through the points were computed by nonlinear regression (see Materials and Methods). This analysis assumes that k_4 is the extent of labeling in the absence of ATP and that ATP competitively inhibits labeling (k_5 is the decrease in labeling produced by saturating ATP levels and K_{iATP} is the concentration of ATP that inhibits labeling half-maximally). The computed constants are as follows: pH 8.0, $k_4 = (1.1 \pm 0.1) \times 10^5$, $k_5 = (1.0 \pm 0.1) \times 10^5$, and $K_{iATP} = 0.5 \pm 0.2$ mM ATP; and pH 5.5, $k_4 = (4.7 \pm 0.3) \times 10^5$, $k_5 = (4.1 \pm 0.5) \times 10^5$, and $K_{iATP} = 1.3 \pm 0.5$ mM ATP.

Table 2: Effect of Reductant on ATP Modulation of Erythrocyte 3OMG Uptake[a]

condition	3OMG uptake (μmol·L cell water^{-1} min^{-1})
control	41.2 ± 7.4
2 mM DTT	57.3 ± 7.1
2 mM ATP	97.7 ± 11.6
2 mM ATP and 2 mM DTT	48.1 ± 3.4

[a] Hypotonically lysed erythrocytes were resealed with or without 2 mM ATP and then incubated with or without 2 mM DTT for 30 min at 37 °C. 3OMG uptake at 100 μM 3OMG was measured at 4 °C. The table summarizes results as the mean ± SEM of three separate experiments made in triplicate.

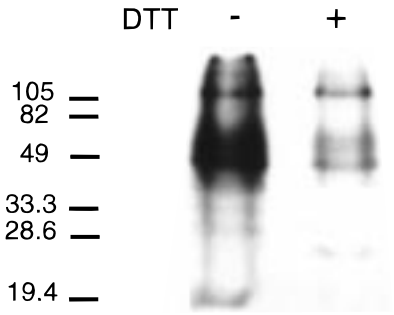

FIGURE 6: Azido[γ-^{32}P]ATP labeling of dimeric and tetrameric GLUT1. Purified GLUT1 was incubated in Tris-HCl medium and 5 mM $MgCl_2$ with or without 4 mM DTT for 30 min at 4 °C. Following labeling with azidoATP, 30 μg samples of protein were resolved on 10% SDS−PAGE minigels. Peptides were transferred to nitrocellulose, and bands containing [γ-^{32}P]ATP were identified by autoradiography. The presence (+) or absence (−) of DTT treatment is indicated above each lane.

labeling are reduced at pH 8.0. The ATP content of erythrocyte ghosts resealed with 4 mM ATP at pH 5.5 or 8.0 is not significantly different (pH 5.5, [ATP] = 3.1 mM; and pH 8.8, [ATP] = 3.1 mM; ATP content of ghosts reasealed in the absence of exogenous ATP, pH 5.5, [ATP] = 0.07 mM; and pH 8.0, [ATP] = 0.069 mM).

Transporter Oligomeric Structure. Erythrocyte-resident GLUT1 exists as a homotetramer but dissociates to form a homodimer upon erythrocyte exposure to extracellular reductant (*21*, *36*). In this study we ask the following question. Does ATP modulate both dimeric and tetrameric GLUT1-mediated sugar transport? Table 2 shows that erythrocyte ghost exposure to reductant (2 mM DTT) inhibits ATP modulation of 3OMG uptake but has no effect on basal uptake measured in the absence of ATP. A reduced capacity to modulate GLUT1-mediated sugar transport in reductant-treated erythrocyte ghosts could result from reduced ATP binding to GLUT1 or from altered interaction of ATP-liganded GLUT1 with regulatory cellular components. Figure 6 shows that incorporation of [γ-^{32}P]ATP into reduced GLUT1 is significantly impaired.

Does ATP Modulate GLUT1-Mediated Sugar Transport Directly?

3-*O*-Methylglucose uptake by reconstituted GLUT1 proteoliposomes is inhibited by cytochalasin B (10 μM) and is stimulated by Mg·ATP (2 mM; Figure 7).

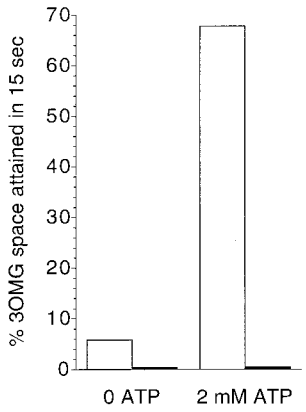

FIGURE 7: ATP stimulates 3OMG uptake into reconstituted, purified GLUT1 proteoliposomes. GLUT1 (100 μg) was reconstituted into eggPC−cholesterol proteoliposomes, and uptake of 50 μM 3OMG was measured at 20 °C in the presence of 5 mM $MgCl_2$ with or without 2 mM ATP, and in the presence or absence of 20 μM cytochalasin B (CB). On the ordinate is the 3OMG uptake expressed as a percentage of the equilibrium 3OMG space of proteoliposomes accessed during 15 s of uptake. On the abscissa is the [ATP] of the medium during reconstitution and uptake determination (0 or 2 mM ATP). Uptake in the presence of CB is shown by the black bars. This figure is representative of three separate experiments.

DISCUSSION

GLUT1 ATP Binding Domain. The results of our peptide mapping studies point to GLUT1 residues 291−364 as the smallest GLUT1 cassette that contains covalently attached [^{32}P]ATP. This result is consistent with previous indirect studies suggesting that GLUT1 residues 270−380 may be involved in nucleotide binding (*25*). This study offers significant improvement over our earlier analyses because we have employed internal markers to indicate the approximate origin of proteolytic fragments previously assigned on the basis of peptide mass and assumed proteolytic enzyme specificity alone. These markers are GLUT1 residues 84−96 (N residues), GLUT1 residues 480−492 (C residues), and asparagine-linked carbohydrate (Asn45). Even using these markers, however, interpretation of GLUT1 peptide mapping studies is complicated by the frequently anomalous mobility of GLUT1 fragments upon SDS−PAGE. For example, a [γ-^{32}P]ATP-labeled EndoLys-C GLUT1 fragment with an intact carboxyl terminus is resolved as a 23 kDa fragment. EndoLys-C specifically hydrolyzes amide, ester, and peptide bonds at the carboxylic side of lysine. If we assume specificity in proteolysis (an assumption supported by sequence analysis of a smaller EndoLys-C GLUT1 fragment), this peptide could derive from cleavage at lysine 300 or lysine 256. The predicted masses of these peptides (21 and 25.8 kDa, respectively) differ significantly from the observed mass.

The smaller [γ-^{32}P]ATP-labeled EndoLys-C GLUT1 fragment (19.1 kDa) was subjected to N-terminal sequence analysis. This confirmed the origin of the [^{32}P]ATP-labeled GLUT1 fragment as Ala301 with hydrolysis occurring at Lys300. If we assume specificity and precise molecular mass determination, this result places the site of [^{32}P]ATP incorporation within a GLUT1 cassette comprised of residues 301−477 (theoretical molecular mass of 19 223 Da). Our peptide mapping studies suggest that [^{32}P]ATP incorporation occurs between GLUT1 residues 291 and 364. This permits further refinement of the azidoATP incorporation domain to residues 301−364. This GLUT1 domain contains primary sequence that is 50% identical with a region of adenylate kinase previously shown to form a hydrophobic strand of a

parallel β-pleated sheet flanking the adenine ribose and triphosphate chain of Mg·ATP (*37*). This sequence

adenylate kinase$_{110\text{-}121}$	GQPTLLLYVDAG
	| || | ||
GLUT1$_{332\text{-}343}$	GRRTLHLIGLAG

is also found in the adenine nucleotide binding proteins glycogen phosphorylase (*38*), RAD3 (*39*), the ATP/ADP translocase (*40*), the human brown fat uncoupling protein (*41*, *42*), phosphofructokinase (*43*), and the α- and β-subunits of F_1-ATPase (*44*). Assignment of this GLUT1 domain to the glucose transport nucleotide-binding pocket, while strengthened by our peptide mapping studies, remains inferential in the absence of a detailed GLUT1 structure. It is interesting to note that GLUT1 also contains the consensus Walker motif GXXXXGKS/T found in a great many ATP and GTP binding proteins (*37*). In GLUT1, this sequence (residues 111−118) may be exposed to the exterior of the cell (*45*), suggesting that it assumes no role in intracellular nucleotide binding.

ATP Affects GLUT1 Function Directly. Isolated GLUT1 is an ATP binding protein. Incorporation of Mg·ATP into the interior of resealed erythrocyte ghosts results in sugar uptake stimulation at subsaturating 3OMG concentrations and produces uptake inhibition at saturating 3OMG concentrations (*25*). Addition of 2 mM Mg·ATP to reconstituted GLUT1 proteoliposomes results in stimulation of 3OMG uptake at subsaturating (50 μM) 3OMG levels. ATP modulations of purified GLUT1- and erythrocyte resident GLUT1-mediated sugar transport are, therefore, fundamentally similar. We conclude that ATP modulation of GLUT1 function requires the presence of only ATP and GLUT1.

This conclusion contrasts with that of Wheeler, who demonstrated that ATP does not modulate the activity of reconstituted human GLUT1 protein (*26*). However, Wheeler's studies employed reduced (DTT-treated) GLUT1 which we have shown to exist as a GLUT1 dimer (*21*). Our studies employ the physiologic, nonreduced form of GLUT1 [a GLUT1 tetramer (*21*)]. We therefore asked two questions. (1) Is reduced GLUT1 susceptible to ATP regulation? (2) Does reduced GLUT1 bind ATP? Our studies show that reductant treatment of erythrocytes converts resident tetrameric GLUT1 to dimeric GLUT1 (*22*), and our findings in this study indicate that reductant also abates ATP modulation of 3OMG transport. Reductant (DTT) treatment of purified GLUT1 results in the loss of azidoATP labeling. These results provide a rational explanation for Wheeler's findings and suggest strongly that dimeric GLUT1 does not present binding sites to nucleotide. They further reinforce the view that red cell-resident GLUT1 exists as the ATP-sensitive GLUT1 tetramer (*22*).

Factors Modulating ATP Regulation of GLUT1. The ATP sensitivity of human erythrocyte sugar transport suggests that regulation of glycolysis and sugar transport in nucleated erythrocytes (*8*, *17*, *46*) and cardiac tissue (*3*, *47*) is coordinated through a common regulatory principle. The major site of glycolytic regulation is phosphofructokinase (PFK) which catalyzes the committed step in glycolysis. PFK is subject to allosteric inhibition by ATP and by citrate and to stimulation by fructose 2,6-bisphosphate and by AMP and ADP (*48*). Pyruvate kinase, the enzyme controlling the out flow from glycolysis, is subject to allosteric inhibition by ATP and to stimulation by fructose 1,6-bisphosphate (*49*, *50*).

Human erythrocyte GLUT1 is subject to allosteric inhibition by ATP (*24*, *25*) which converts low-affinity high-capacity net sugar uptake to high-affinity low-capacity uptake. Maximum rates of exchange transport and net sugar exit appear to be unaffected by cellular ATP levels (*24*). In this study, ATP reduces V_{max} and $K_{m(app)}$ for net 3OMG uptake in erythrocytes at the temperature of ice from 1069 ± 84 μmol per liter of cell water per minute and 12.3 ± 0.8 mM to 220 ± 19 μmol per liter of cell water per minute and 386 ± 24 μM, respectively. ATP thus increases the ratio $V_{max}/K_{m(app)}$ by some 5−6-fold. This is not markedly different from the 3-fold increase reported previously (*24*). The net effect of ATP on 3OMG uptake at subsaturating sugar levels (50−100 μM) is stimulation of transport by a factor proportional to the increase in the ratio $V_{max}/K_{m(app)}$, while transport at 3OMG levels greater than $K_{m(app)}$ (saturated transport) is inhibited.

We examined whether ATP regulation of transport in resealed ghosts is subject to modulation by glycolytic intermediates known to regulate glycolysis. Only AMP antagonizes the action of ATP on 3OMG uptake. Citrate, fructose 1,6-bisphosphate, and fructose 2,6-bisphosphate (key regulators of PFK or pyruvate kinase) have no effect on basal or ATP-stimulated sugar uptake. Other intermediates were similarly inactive. ADP, however, mimics the ability of ATP to modulate transport. These effects of AMP and ADP on sugar transport in erythrocyte ghosts are similar to those reported previously (*25*). External application of ADP inhibits ATP modulation of sugar efflux from inside out erythrocyte membranes vesicles and, like AMP, antagonizes the action of ATP to slow C-Ab binding to purified GLUT1 (*25*). This suggests that residual adenylate kinase present in erythrocyte ghosts converts ADP to ATP, a hypothesis supported by ATP assays of ADP-loaded ghosts (*25*). We conclude, therefore, that ATP regulation of sugar transport is subject to inhibition by AMP and possibly by ADP. The glucose transporter, an enzyme of glycolysis, is characteristically sensitive to the energy charge of the cell.

All experiments used to investigate the action of glycolytic intermediates on ATP modulation of sugar transport were performed at a fixed pH (7.4). Under normal circumstances, increased glycolytic flux gives rise to elevated lactic acid levels and reduced pH (*34*, *51*, *52*). We therefore examined the effect of altered pH on basal and ATP-regulated sugar transport. To our surprise, we observed that while reduced pH inhibited ATP modulation of sugar transport, the level of azido[γ-^{32}P]ATP labeling of GLUT1 was increased. Reduced pH serves to increase both the level of maximum photoincorporation of [γ-^{32}P]ATP and $K_{i(app)}$ for ATP inhibition of photolabeling. ATP stimulation of transport at pH 8.0 increases in a saturable manner with nucleotide concentration. However, ATP stimulation of transport at pH 5.5 increases with nucleotide concentrations up to 200 μM and thereafter falls with increasing ATP. ATP assays indicate that intracellular ATP is not degraded to a significantly greater extent at low pH. Computation of free Mg^{2+}, ATP, and Mg·ATP levels indicates that these observations are not explained by systematic (pH-dependent) changes in these species. We conclude that intracellular ATP exerts antago-

nistic actions on sugar transport at pH 5.5. The nature of the inhibitory action is presently unknown. An increased level of GLUT1 labeling by azidoATP at reduced pH raises the possibility that a unique, transport-antagonistic ATP binding site is revealed at acidic pH. Future studies must address this possibility.

Relationship to Sugar Transport Regulation in Other Tissues. Sugar transport in avian erythrocytes is subject to regulation by cellular metabolic status. Under basal conditions, protein-mediated net sugar uptake is barely detectable. Exposure to anoxia or to inhibitors of oxidative metabolism results in a robust stimulation of net sugar uptake (*6*, *7*). Recent studies have demonstrated that avian erythrocyte GLUT1 is present at the cell surface at all times (*17*) but functions as an antiporter in basal cells (*18*). This means that sugar uptake proceeds only when it is coupled to sugar exit. Following metabolic disruption, avian red cell GLUT1 can now catalyze sugar uniport (*18*), allowing net sugar uptake in the absence of intracellular sugar. Antiport function appears to be unaffected by cellular metabolic status.

While avian erythrocyte GLUT1-mediated sugar uniport is controlled more completely by cellular metabolic status than is human erythrocyte sugar uniport, the similarity between transport regulation in both tissues is striking. GLUT1-mediated uniport but not exchange (antiport) is accelerated under conditions of cellular ATP depletion. Uniport function requires that the transporter undergo a full catalytic cycle in the absence of sugar at one or even both sides of the membrane (*53*, *54*). Exchange function represents only one-half of the transporter's catalytic cycle in which conformational changes can proceed exclusively when the substrate is bound to the carrier. Our findings suggest that those substrate-independent GLUT1 conformational changes that are necessary to complete the full catalytic cycle and thereby permit uniport function are strongly inhibited when ATP is bound to GLUT1. It is noteworthy that the GLUT1 carboxyl terminus is less accessible to peptide-directed antibodies under conditions where uniport is inhibited [in the presence of ATP (*25*)]. In addition, the GLUT1 carboxyl terminus truncation prevents substrate-independent conformational changes necessary for uniport (*55*, *56*). It is interesting to speculate, therefore, that conformational changes in the GLUT1 carboxyl terminus control antiport−uniport switching and that this, in turn, is regulated by ATP binding to GLUT1.

ATP Regulation of GLUT1 in Erythrocytes. Saturating intracellular ATP reduces V_{max} for net uptake by 90% (*18*). The consequences of GLUT1 allosteric interaction with ATP, ADP, and AMP on net glucose transport can be predicted assuming nucleotide interactions with GLUT1 are mutually competitive and that AMP and ADP antagonize the effect of ATP on net sugar uptake (*25*). Human erythrocyte AMP, ADP, and ATP levels are approximately 2.6 mM, 0.14 mM, and 12 μM, respectively (*57*). K_d for ATP binding to GLUT1 at pH 8 is 0.5 mM (Figure 5), while $K_{i(app)}$ values for AMP and ADP inhibition of ATP binding to GLUT1 are 120 and 80 μM, respectively (*25*). $K_{d(app)}$ for ATP binding to GLUT1 in the presence of ADP and AMP is given by

$$K_{d(app)} = K_d\left(1 + \frac{[AMP]}{K_{dAMP}} + \frac{[ADP]}{K_{dADP}}\right)$$

Under the prevailing nucleotide conditions, $K_{d(app)}$ equals 1.4 mM ATP, the transporter is 65% saturated by ATP, and V_{max} for net sugar uptake is inhibited by 59%. If ATP levels were to fall 20% and ADP and AMP levels were to increase 30- and 50-fold, respectively, as in a hypoxic heart (*58*, *59*), $K_{d(app)}$ would equal 29 mM ATP, the transporter would be 7% saturated by ATP, and V_{max} for net sugar uptake would be inhibited by only 6%. The result would be a 2.3-fold increase in net uptake during metabolic inhibition.

Erythrocytes also contain high levels of reduced glutathione [approximately 4 mM (*60*)]. While reductant causes tetrameric GLUT1 to dissociate into GLUT1 dimers (*22*) and thereby lose allosteric regulation by ATP, reductant acts only at an extracellular site (*22*). GLUT1 quaternary structure and regulation by ATP are, therefore, unaffected by intracellular reductant.

Conclusions. Upon assembly into its native tetrameric form, human erythrocyte GLUT1 is an adenine nucleotide binding protein. GLUT1 residues 301−364 are closely associated with the nucleotide binding domain. When it is liganded by ATP, the net sugar import capacity of tetrameric GLUT1 is reduced 5-fold. Intracellular AMP and acidification antagonize the inhibitory action of ATP on net import. ATP modulates sugar transport in reconstituted, tetrameric GLUT1 proteoliposomes, indicating that GLUT1 and ATP are sufficient for transport regulation. Our studies suggest that dimeric GLUT1 neither binds nor is modulated by ATP.

REFERENCES

1. Mueckler, M. (1994) *Eur. J. Biochem. 219*, 713−725.
2. Elbrink, J., and Bihler, I. (1975) *Science 188*, 1177−1184.
3. Haworth, R. A., and Berkoff, H. A. (1986) *Circ. Res. 58*, 157−165.
4. Lee, A. D., Hansen, P. A., and Holloszy, J. O. (1995) *FEBS Lett. 361*, 51−54.
5. Hansen, P., Gulve, E., Gao, J., Schluter, J., Mueckler, M., and Holloszy, J. (1995) *Am. J. Physiol. 268*, C30−C35.
6. Cheung, J. Y., Regen, D. M., Schworer, M. E., Whitfield, C. F., and Morgan, H. E. (1977) *Biochim. Biophys. Acta 470*, 212−229.
7. Simons, T. J. B. (1983) *J. Physiol. (London) 338*, 501−526.
8. Whitfield, C. F., and Morgan, J. E. (1983) *Biochim. Biophys. Acta 307*, 181−196.
9. Douen, A. G., Ramlal, T., Rastogi, S., Bilan, P. J., Cartee, G. D., Vranic, M., Holloszy, J. O., and Klip, A. (1990) *J. Biol. Chem. 265*, 13427−13430.
10. Gao, J., Ren, J., Gulve, E. A., and Holloszy, J. O. (1994) *J. Appl. Physiol. 77*, 1597−1601.
11. Wang, W., Hansen, P. A., Marshall, B. A., Holloszy, J. O., and Mueckler, M. (1996) *J. Cell Biol. 135*, 415−430.
12. Doria, M. C., Lund, D. D., Pasley, A., Sandra, A., and Sivitz, W. I. (1993) *Am. J. Physiol. 265*, E454−E464.
13. Kolter, T., Uphues, I., Wichelhaus, A., Reinauer, H., and Eckel, J. (1992) *Biochem. Biophys. Res. Commun. 189*, 1207−1214.
14. Sun, D., Nguyen, N., DeGrado, T. R., Schwaiger, M., and Brosius, F. C. r. (1994) *Circulation 89*, 793−798.
15. Wheeler, T. J., Fell, R. D., and Hauck, M. A. (1994) *Biochim. Biophys. Acta 1196*, 191−200.
16. Fischer, Y., Thomas, J., Rosen, P., and Kammermeier, H. (1995) *Endocrinology 136*, 412−420.
17. Diamond, D., and Carruthers, A. (1993) *J. Biol. Chem. 268*, 6437−6444.
18. Cloherty, E. K., Diamond, D. L., Heard, K. S., and Carruthers, A. (1996) *Biochemistry 35*, 13231−13239.
19. Mueckler, M., Caruso, C., Baldwin, S. A., Panico, M., Blench, I., Morris, H. R., Allard, W. J., Lienhard, G. E., and Lodish, H. F. (1985) *Science 229*, 941−945.

20. Wheeler, T. J., and Hinkle, P. C. (1985) *Annu. Rev. Physiol. 47*, 503−518.
21. Hebert, D. N., and Carruthers, A. (1992) *J. Biol. Chem. 267*, 23829−23838.
22. Zottola, R. J., Cloherty, E. K., Coderre, P. E., Hansen, A., Hebert, D. N., and Carruthers, A. (1995) *Biochemistry 34*, 9734−9747.
23. Cloherty, E. K., Heard, K. S., and Carruthers, A. (1996) *Biochemistry 35*, 10411−10421.
24. Helgerson, A. L., Hebert, D. N., Naderi, S., and Carruthers, A. (1989) *Biochemistry 28*, 6410−6417.
25. Carruthers, A., and Helgerson, A. L. (1989) *Biochemistry 28*, 8337−8346.
26. Wheeler, T. J. (1989) *Biochemistry 28*, 3413−3420.
27. Sogin, D. C., and Hinkle, P. C. (1980) *Proc. Natl. Acad. Sci. U.S.A. 77*, 5725−5729.
28. Carruthers, A. (1986) *J. Biol. Chem. 261*, 11028−11037.
29. Laemmli, U. K. (1970) *Nature 270*, 680−685.
30. Bers, D. M., Patton, C. W., and Nuccitelli, R. (1994) *Methods Cell Biol. 40*, 3−29.
31. Martell, A. E., and Smith, R. M. (1974) *Critical Stability Constants*, Plenum Press, New York.
32. Smith, B. L., and Agre, P. (1991) *J. Biol. Chem. 266*, 6407−6415.
33. Jekel, P. A., Weijer, W. J., and Beintema, J. J. (1983) *Anal. Biochem. 134*, 347−354.
34. Cairns, S. P., Westerblad, H., and Allen, D. G. (1993) *J. Physiol. (London) 464*, 561−574.
35. Sen, A. K., and Widdas, W. F. (1962) *J. Physiol. (London) 160*, 392−403.
36. Zottola, R. J., Cloherty, E. K., Coderre, P. E., Hansen, A., Hebert, D. N., and Carruthers, A. (1995) *Biochemistry 34*, 9734−9747.
37. Fry, D. C., Kuby, S. A., and Mildvan, A. S. (1986) *Proc. Natl. Acad. Sci. U.S.A. 83*, 907−911.
38. Newgard, C. B., Littman, D. R., van Genderen, C., Smith, M., and Fletterick, R. J. (1988) *J. Biol. Chem. 263*, 3850−3857.
39. Reynolds, P., Higgins, D. R., Prakash, L., and Prakash, S. (1985) *Nucleic Acids Res. 13*, 2357−2372.
40. Plano, G. V., and Winkler, H. H. (1991) *J. Bacteriol. 173*, 3389−3396.
41. Cassard, A. M., Bouillaud, F., Mattei, M. G., Hentz, E., Raimbault, S., Thomas, M., and Ricquier, D. (1990) *J. Cell. Biochem. 43*, 255−264.
42. Casteilla, L., Bouillaud, F., Forest, C., and Ricquier, D. (1989) *Nucleic Acids Res. 17*, 2131.
43. Valdez, B. C., Chen, Z., Sosa, M. G., Younathan, E. S., and Chang, S. H. (1989) *Gene 76*, 167−169.
44. Ohta, S., and Kagawa, Y. (1986) *J. Biochem. (Tokyo) 99*, 135−141.
45. Hresko, R. C., Kruse, M., Strube, M., and Mueckler, M. (1994) *J. Biol. Chem. 269*, 20482−20488.
46. Wood, R. E., and Morgan, H. E. (1969) *J. Biol. Chem. 244*, 1451−1460.
47. Mansford, K. R. (1968) *Proc. R. Soc. Med. 61*, 816−819.
48. Carpenter, J. F., and Hand, S. C. (1986) *Arch. Biochem. Biophys. 248*, 1−9.
49. Rosevear, P. R., Fox, T. L., and Mildvan, A. S. (1987) *Biochemistry 26*, 3487−3493.
50. Waygood, E. B., Mort, J. S., and Sanwal, B. D. (1976) *Biochemistry 15*, 277−282.
51. Elliott, A. C., Smith, G. L., Eisner, D. A., and Allen, D. G. (1992) *J. Physiol. (London) 454*, 467−490.
52. Smith, G. L., Donoso, P., Bauer, C. J., and Eisner, D. A. (1993) *J. Physiol. (London) 472*, 11−22.
53. Stein, W. D. (1986) *Transport and diffusion across cell membranes*, Academic Press, New York.
54. Carruthers, A. (1991) *Biochemistry 30*, 3898−3906.
55. Due, A. D., Qu, Z. C., Thomas, J. M., Buchs, A., Powers, A. C., and May, J. M. (1995) *Biochemistry 34*, 5462−5471.
56. Oka, Y., Asano, T., Shibasaki, Y., Lin, J. L., Tsukuda, K., Katagiri, H., Akanuma, Y., and Takaku, F. (1990) *Nature 345*, 550−553.
57. Formato, M., Masala, B., and De Luca, G. (1990) *Clin. Chim. Acta 189*, 131−137.
58. Lavanchy, N., Grably, S., Garnier, A., and Rossi, A. (1996) *Mol. Cell. Biochem. 160−161*, 273−282.
59. Allen, D. G., Morris, P. G., Orchard, C. H., and Pirolo, J. S. (1985) *J. Physiol. (London) 361*, 185−204.
60. Beutler, E., Gelbart, T., and Pegelow, C. (1986) *J. Clin. Invest. 77*, 38−41.

BI980585Y